

REVIEW OF SOLAR AND REACTOR NEUTRINOS

A. W. P. POON

Institute for Nuclear and Particle Astrophysics, Nuclear Science Division

Lawrence Berkeley National Laboratory

1 Cyclotron Road, Berkeley, CA 94720, USA

E-mail: awpoon@lbl.gov

Over the last several years, experiments have conclusively demonstrated that neutrinos are massive and that they mix. There is now direct evidence for ν_e s from the Sun transforming into other active flavors while en route to the Earth. The disappearance of reactor $\bar{\nu}_e$ s, predicted under the assumption of neutrino oscillation, has also been observed. In this paper, recent results from solar and reactor neutrino experiments and their implications are reviewed. In addition, some of the future experimental endeavors in solar and reactor neutrinos are presented.

1 Introduction

From the 1960s to just a few years ago, solar neutrino experiments had been observing fewer neutrinos than what were predicted by detail models of the Sun^{1,2,3,4,5,6}. The radiochemical experiments, which used ^{37}Cl ⁷ and ^{71}Ga ^{8,9,10} as targets, were sensitive exclusively to ν_e . The real-time water Cherenkov detector Super-Kamiokande^{11,12,13,14} (and its predecessor Kamiokande¹⁵) observes solar neutrinos by ν -e elastic scattering, and has sensitivity to all active neutrino flavors. However, its sensitivity to ν_μ and ν_τ is only 1/6 of that for ν_e , and the flavor content of the observed solar neutrino events cannot be determined.

As these terrestrial detectors have different kinematic thresholds, they probed different parts of the solar neutrino energy spectrum. The measured solar neutrino flux exhibited an energy dependence. These observations of an energy dependent flux deficit can be explained only if the solar models are incomplete or neutrinos undergo flavor transformation while in transit to the Earth. Table 1 shows a comparison of the predicted and the observed solar neutrino fluxes for these experiments.

Since 2001, significant advances have been made in solar neutrino physics. The Sudbury Neutrino

Observatory (SNO)^{16,17,18,19,20,21} has conclusively demonstrated that a significant fraction of ν_e s that are produced in the solar core transforms into other active flavors. One of the most favored explanation for this flavor transformation is matter-enhanced neutrino oscillation, or the Mikheyev-Smirnov-Wolfenstein (MSW) effect²⁵. The KamLAND experiment^{22,23,24} observes the disappearance of reactor $\bar{\nu}_e$ s that is predicted from the neutrino mixing parameters derived from global MSW analyses of solar neutrino results. This provides very strong evidence that MSW oscillation is the underlying mechanism in solar neutrino flavor transformation. In this paper, these advances in solar and reactor neutrino experiments and their physical implications are discussed. A brief overview of the future program in solar neutrinos and reactor anti-neutrinos will also be presented.

2 Solar Neutrino Flux Measurements at Super-Kamiokande

The Super-Kamiokande (SK) detector is a 50000-ton water Cherenkov detector located in the Kamioka mine, Gifu prefecture, Japan. During the first phase of the experiment SK-I (April 1996 to July 2001), approximately 11200 20-inch-diameter photomulti-

Table 1. Summary of solar neutrino observations at different terrestrial detectors before 2002. The Bahcall-Pinsonneault (BP2001) model predictions of the solar neutrino flux are presented in this table. The experimental values are shown with statistical uncertainties listed first, followed by systematic uncertainties. The Solar Neutrino Unit (SNU) is a measure of solar neutrino interaction rate, and is defined as 1 interaction per 10^{-36} target atom per second. For the Kamiokande and Super-Kamiokande experiments, the predicted and measured neutrino fluxes are listed in units of $10^6 \text{ cm}^{-2} \text{ s}^{-1}$.

Experiment	Measured Rate/Flux	SSM Prediction (BP2001) ¹
Homestake ⁷ (³⁷ Cl)	$2.56 \pm 0.16 \pm 0.16$ SNU	$7.6^{+1.3}_{-1.1}$ SNU
SAGE ⁸ (⁷¹ Ga)	$70.8^{+5.3}_{-5.2} \pm 3.7_{-3.2}$ SNU	
Gallex ⁹ (⁷¹ Ga)	$77.5 \pm 6.2^{+4.3}_{-4.7}$ SNU	128^{+9}_{-7} SNU
GNO ¹⁰ (⁷¹ Ga)	$62.9^{+5.5}_{-5.3} \pm 2.5$ SNU	
Kamiokande ¹⁵ (νe)	$2.80 \pm 0.19 \pm 0.33$	$5.05 (1^{+0.20}_{-0.16})$
Super-Kamiokande ¹² (νe)	$2.32 \pm 0.03^{+0.08}_{-0.07}$	

plier tubes (PMTs) were mounted on a cylindrical tank to detect Cherenkov light from neutrino interactions in the inner detector. Since December 2002, the experiment has been operating in its second phase (SK-II) with approximately 5200 PMTs in its inner detector. An additional 1885 8-inch-diameter PMTs are used as a cosmic veto.

2.1 Super-Kamiokande-I

In SK-I and SK-II, neutrinos from the Sun are detected through the elastic scattering process $\nu e \rightarrow \nu e$. Because of the strong directionality in this process, the reconstructed direction of the scattered electron is strongly correlated to the direction of the incident neutrinos. The sharp elastic scattering peak in the angular distribution for events with a total electron energy of $5 < E < 20$ MeV in the SK-I data set is shown in Figure 1. This data set spans 1496 days (May 31, 1996 to July 15, 2001), and the solar neutrino flux is extracted by statistically separating the solar neutrino signal and the backgrounds using this angular distribution. At the analysis threshold of $E=5$ MeV, the primary signal is $\nu_e s$ from ⁸B decays in the solar interior. The extracted solar ⁸B neutrino flux in this SK-I data set ($\phi_{\text{SK-I}}^{\text{ES}}$) is²⁶ (in units of $10^6 \text{ cm}^{-2} \text{ s}^{-1}$):

$$\phi_{\text{SK-I}}^{\text{ES}} = 2.35 \pm 0.02(\text{stat.}) \pm 0.08(\text{sys.})$$

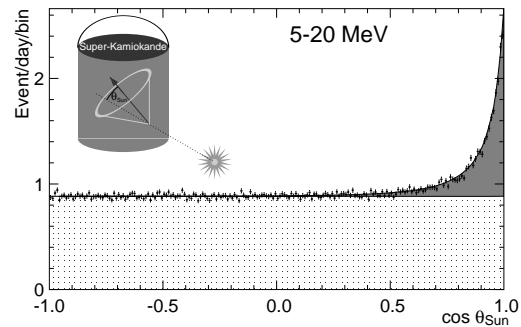


Figure 1. Angular distribution of solar neutrino event candidates in the 1496-day SK-I data set. The shaded area is the solar neutrino elastic scattering peak, and the dotted area represents backgrounds in the candidate data set.

When comparing this measured flux to the BP2001¹ and BP2004² model predictions:

$$\frac{\phi_{\text{SK-I}}^{\text{ES}}}{\phi_{\text{BP2001}}} = 0.465 \pm 0.005(\text{stat.})^{+0.016}_{-0.015}(\text{sys.})$$

$$\frac{\phi_{\text{SK-I}}^{\text{ES}}}{\phi_{\text{BP2004}}} = 0.406 \pm 0.004(\text{stat.})^{+0.014}_{-0.013}(\text{sys.}),$$

where the model uncertainties ($\sim 20\%$) have not been included in the systematic uncertainties above.

2.2 Super-Kamiokande-II

With only about half of the photocathode coverage as SK-I, significant improvements have been made to the trigger system in the SK-II detector in order to maintain high

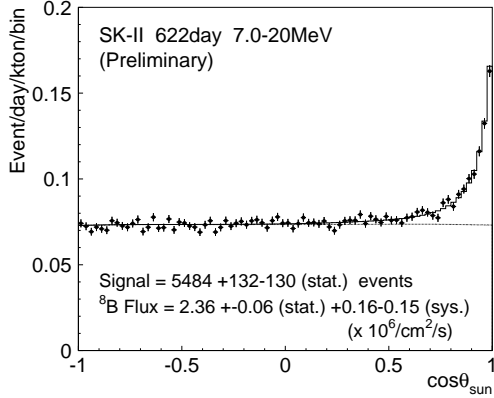


Figure 2. Angular distribution of solar neutrino event candidates in a 622-day data set in SK-II. For the first 159 days of these data, the energy threshold for the analysis was set at $E = 8$ MeV, and it was lowered to 7 MeV for the remaining 463 days of data.

trigger efficiency for solar neutrino events. The improved trigger system can trigger with 100% efficiency at $E \sim 6.5$ MeV. Results from a 622-day SK-II data set have recently been released. The solar angular distribution plot is shown in Figure 2. For the first 159 days (Dec. 24, 2002 to July 15, 2003) of these data, the energy threshold for the analysis was set at $E = 8$ MeV, and it was lowered to 7 MeV for the remaining 463 days (Jul. 15, 2003 to Mar. 19, 2005). The extracted solar ^8B neutrino flux in this 622-day SK-II data set ($\phi_{\text{SK-II}}^{\text{ES}}$) is (in units of $10^6 \text{ cm}^{-2} \text{ s}^{-1}$):

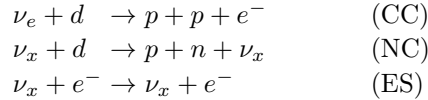
$$\phi_{\text{SK-II}}^{\text{ES}} = 2.36 \pm 0.06(\text{stat.})_{-0.15}^{+0.16}(\text{sys.}),$$

which is consistent with the SK-I results.

3 Sudbury Neutrino Observatory

The Sudbury Neutrino Observatory (SNO) detector is a 1000-tonne heavy water (D_2O) Cherenkov detector located near Sudbury, Ontario, Canada. Approximately 9500 8-inch-diameter PMTs are mounted on a spherical geodesic structure to detect Cherenkov light resulting from neutrino interactions. It can make simultaneous measurements of the ν_e flux from ^8B decay in the Sun and the flux

of all active neutrino flavors²⁷ through the following reactions:



The charged-current (CC) reaction on the deuteron is sensitive exclusively to ν_e , and the neutral-current (NC) reaction has equal sensitivity to all active neutrino flavors (ν_x , $x = e, \mu, \tau$). Similar to the Super-Kamiokande experiment, elastic scattering (ES) on electron is also sensitive to all active flavors, but with reduced sensitivity to ν_μ and ν_τ . If the measured total ν_x flux (through the NC channel) is greater than the measured ν_e flux (through the CC channel), it would conclusively demonstrate that solar ν_e s have undergone flavor transformation since their production in the solar core. Alternatively, this flavor transformation can be demonstrated by comparing the ν_x flux deduced from the ES channel to the ν_e flux.

3.1 Pure D_2O phase

The first phase of the SNO experiment (SNO-I) used a pure D_2O target. The free neutron from the NC interaction is thermalized, and in 30% of the time, a 6.25-MeV γ ray is emitted following the neutron capture by deuteron. In 2001, the SNO collaboration published a measurement of the ν_e flux, based on a 241-day data set taken from Nov. 2, 1999 to Jan 15, 2001. At an electron kinetic energy T_{eff} threshold of 6.75 MeV¹⁷, the measured ν_e and ν_x fluxes through the CC $\phi_{\text{SNO-I}}^{\text{CC}}$ and ES $\phi_{\text{SNO-I}}^{\text{ES}}$ channels are (in units of $10^6 \text{ cm}^{-2} \text{ s}^{-1}$):

$$\begin{aligned} \phi_{\text{SNO-I}}^{\text{CC}} &= 1.75 \pm 0.07(\text{stat.})_{-0.11}^{+0.12}(\text{sys.}) \\ \phi_{\text{SNO-I}}^{\text{ES}} &= 2.39 \pm 0.34(\text{stat.})_{-0.14}^{+0.16}(\text{sys.}). \end{aligned}$$

The measured $\phi_{\text{SNO-I}}^{\text{ES}}$ agrees with that from the SK-I detector $\phi_{\text{SK-I}}^{\text{ES}}$. But a comparison of $\phi_{\text{SNO-I}}^{\text{CC}}$ to $\phi_{\text{SK-I}}^{\text{ES}}$, after adjusting for the difference in the energy response of the two

detectors, yields (in units of $10^6 \text{ cm}^{-2}\text{s}^{-1}$)

$$\phi_{\text{SK-I}}^{\text{ES}}(\nu_x) - \phi_{\text{SNO-I}}^{\text{ES}}(\nu_e) = 0.57 \pm 0.17,$$

which is 3.3σ away from 0. This measurement not only confirmed previous observations of the solar neutrino deficit from different experiments, it also provided the first indirect evidence, when combined with the SK-I results, that neutrino flavor transformation might be the solution to this long-standing deficit.

In 2002, the SNO collaboration reported a measurement of the total active neutrino flux through the NC channel¹⁸. This measurement used a T_{eff} threshold of 5 MeV and was based the 306-day data set (Nov. 2, 1999 to May 28, 2001). Under the assumption of an undistorted ${}^8\text{B}$ ν_e spectrum, the non- ν_e component ($\phi_{\text{SNO-I}}^{\mu\tau}$) of the total active neutrino flux is (in units of $10^6 \text{ cm}^{-2}\text{s}^{-1}$)

$$\phi_{\text{SNO-I}}^{\mu\tau} = 3.41 \pm 0.45(\text{stat.})_{-0.45}^{+0.48}(\text{sys.}),$$

which is 5.3σ away from 0. This result was the first direct evidence that demonstrated neutrino flavor transformation. The measured total active neutrino flux confirmed the solar model predictions and provided the definitive solution to the solar neutrino deficit problem.

3.2 Salt Phase

In phase two of the SNO experiment (SNO-II), 2 tonnes of NaCl were added to the D_2O target in order to enhance the detection efficiency of the NC channel. The free neutron from the NC channel was thermalized in the D_2O and subsequently captured by a ${}^{35}\text{Cl}$ nucleus, which resulted in the emission of a γ -ray cascade with a total energy of 8.6 MeV. The neutron capture efficiency increased three folds from SNO-I. The CC signal involved a single electron and multiple γ s were emitted in the NC channel. This difference in the number of particles in the final state resulted in a difference in the isotropy of the Cherenkov light distribution. The CC

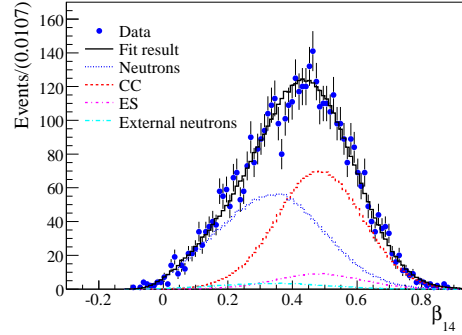


Figure 3. Statistical separation of CC and NC events using Cherenkov light isotropy in SNO-II. The measure of isotropy, β_{14} , is a function with Legendre polynomials of order 1 and 4 as its bases. Because there were multiple γ s in the NC signal, the Cherenkov light distribution was more diffuse (smaller β_{14}).

and the NC signals could be statistically separated by this isotropy difference. This separation for events with $T_{\text{eff}} > 5.5$ MeV is shown in Fig. 3 for the 391-day data set (taken from Jul. 26, 2001 to Aug. 28, 2003). This use of light isotropy also removed the need to constrain the ${}^8\text{B}$ ν_e energy spectrum, which can be distorted if the neutrino flavor transformation process is energy dependent, as in SNO-I. The measured energy-unconstrained ν_e and ν_x fluxes through the different channels are^{20,21} (in units of $10^6 \text{ cm}^{-2}\text{s}^{-1}$):

$$\phi_{\text{SNO-II}}^{\text{uncon.CC}} = 1.68 \pm 0.06(\text{stat.})_{-0.09}^{+0.08}(\text{sys.})$$

$$\phi_{\text{SNO-II}}^{\text{uncon.ES}} = 2.35 \pm 0.22(\text{stat.})_{-0.15}^{+0.15}(\text{sys.})$$

$$\phi_{\text{SNO-II}}^{\text{uncon.NC}} = 4.94 \pm 0.21(\text{stat.})_{-0.34}^{+0.38}(\text{sys.}).$$

The ratio of the ν_e flux and the total active neutrino flux is of physical significance (which will be discussed later), and is

$$\frac{\phi_{\text{SNO-II}}^{\text{uncon.CC}}}{\phi_{\text{SNO-II}}^{\text{uncon.NC}}} = 0.340 \pm 0.023(\text{stat.})_{-0.031}^{+0.029}(\text{sys.}).$$

4 Search for MSW Signatures in Solar Neutrinos

Recent results from SNO and Super-Kamiokande have conclusively

demonstrated that neutrino flavor transformation is the solution to the solar neutrino deficit. The most favored mechanism for this transformation is the Mikheyev-Smirnov-Wolfenstein (MSW) matter-enhanced neutrino oscillation²⁵. MSW oscillation can be a resonant effect as opposed to vacuum oscillation, which is simply the projection of the time evolution of eigenstates in free space. A resonant conversion of ν_e to other active flavors is possible in MSW oscillation if the ambient matter density matches the resonant density. Two distinct signatures of the MSW effect are distortion of the neutrino energy spectrum and a day-night asymmetry in the measured neutrino flux. The former signature arises from the energy dependence in neutrino oscillation. When the Sun is below a detector's horizon, some of the oscillated solar neutrinos may revert back to ν_e while traversing the Earth's interior. This ν_e regeneration effect would give an asymmetry in the measured ν_e fluxes during the day and the night.

Both SNO and Super-Kamiokande have done extensive searches for these two signatures in their data. Figure 4 shows the measured electron spectra from SK-I and SK-II, whereas Fig. 5 shows the measured spectra from SNO-I and SNO-II. No statistically significant distortion is seen from either experiment.

The Super-Kamiokande experiment defines the day-night asymmetry ratio $A_{\text{DN}}^{\text{SK}}$ as¹⁴

$$A_{\text{DN}}^{\text{SK}} = \frac{\Phi_{\text{D}} - \Phi_{\text{N}}}{\frac{1}{2}(\Phi_{\text{D}} + \Phi_{\text{N}})},$$

where Φ_{D} is the measured neutrino flux when the Sun is above the horizon, and Φ_{N} is the corresponding flux when the Sun is below the horizon. The measured day-night asymmetries of the solar neutrino flux by SK-I and SK-II are:

$$A_{\text{DN}}^{\text{SK-I}} = -0.021 \pm 0.020(\text{stat.})_{-0.012}^{+0.013}(\text{sys.})$$

$$A_{\text{DN}}^{\text{SK-II}} = 0.014 \pm 0.049(\text{stat.})_{-0.025}^{+0.024}(\text{sys.}).$$

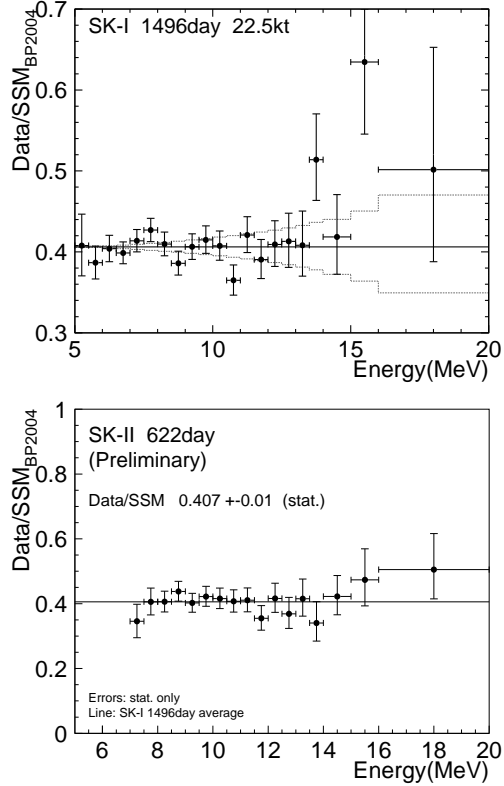


Figure 4. Measured electron energy spectra from SK-I and SK-II. The measured spectra have been normalized to the BP2004 model predictions. The solid lines indicate the mean of the measured ^8B neutrino flux. The band in the SK-I spectrum represents the energy-correlated systematic uncertainties in the measurement.

It should be noted that the flux measured by Super-Kamiokande is a mixture of all three active neutrino flavors.

The SNO experiment has also measured the day-night asymmetry of the measured neutrino flux^{19,21}. It should be noted that the SNO and the Super-Kamiokande asymmetry ratios are defined differently, such that $A_{\text{DN}}^{\text{SNO}} = -A_{\text{DN}}^{\text{SK}}$. Because SNO can measure the ν_e flux and the total active neutrino flux separately through the CC and the NC channels, it can determine the day-night asymmetry for these fluxes separately. In addition, the asymmetry ratio can be determined with the day-night asymmetry in the NC channel

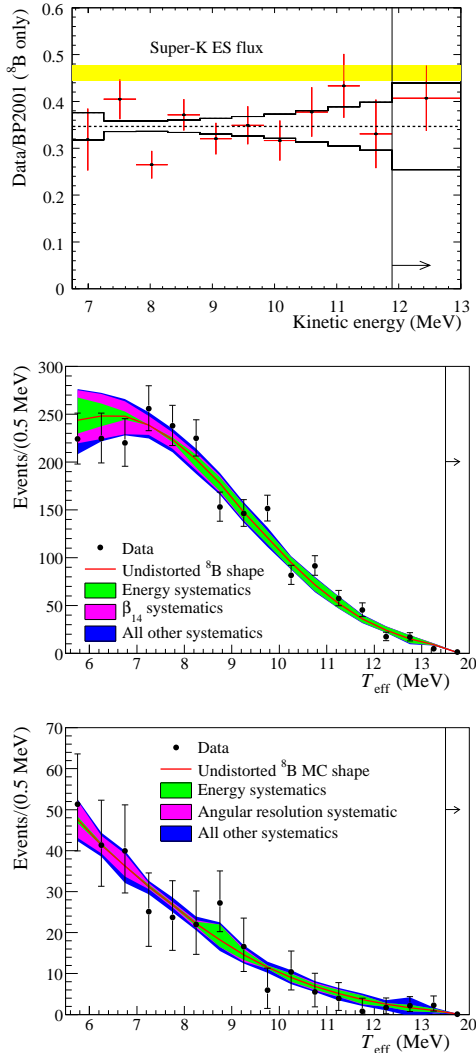


Figure 5. Measured electron energy spectra from SNO-I and SNO-II. *Top*: The ratio of the measured SNO-I CC electron kinetic energy spectrum to the expected undistorted kinetic energy distribution for ^8B neutrinos (in BP2001 model) with correlated systematic uncertainties. *Middle*: The measured CC electron kinetic energy spectrum in SNO-II is shown as the data points (with statistical uncertainties only). *Bottom*: The measured ES electron kinetic energy spectrum in SNO-II is shown as the data points (with statistical uncertainties only). In the last two plots, the bands show the accumulated effect of different correlated systematic uncertainties on the electron spectra expected from an undistorted ^8B neutrino spectrum.

$A_{\text{NC,DN}}^{\text{SNO}}$ constrained to 0. With the ^8B shape and $A_{\text{NC,DN}}^{\text{SNO}} = 0$ constraints, the measured day-night asymmetry in the ν_e flux in SNO-I and SNO-II are

$$A_{e,\text{DN}}^{\text{SNO-I}} = 0.021 \pm 0.049(\text{stat.})_{-0.012}^{+0.013}(\text{sys.})$$

$$A_{e,\text{DN}}^{\text{SNO-II}} = -0.015 \pm 0.058(\text{stat.})_{-0.027}^{+0.027}(\text{sys.}).$$

Because of the presence of ν_μ and ν_τ in the Super-Kamiokande measured flux, its day-night asymmetry is diluted by a factor of 1.55^{21} . Assuming an energy-independent conversion mechanism and only active neutrinos, the SK-I result scales to a ν_e flux asymmetry $A_{e,\text{SK-I}} = 0.033 \pm 0.031_{-0.020}^{+0.019}$. Combining the SNO-I and SNO-II values for $A_{e,\text{DN}}$ with the equivalent SK-I value ($A_{e,\text{SK-I}}$) gives $A_{e,\text{combined}} = 0.035 \pm 0.027$. No statistically significant day-night asymmetry has been observed.

5 MSW Interpretation of Solar Neutrino Data

Although no direct evidence for the MSW effect has been observed, the null hypothesis that no MSW oscillation in the solar neutrino results is rejected at $5.6\sigma^{28}$. There are two parameters in a two-flavor, active neutrino oscillation model: Δm^2 , which is the difference of between the square of the eigenvalue of two neutrino mass states; and $\tan^2 \theta$, which quantifies the mixing strength between the flavor and the mass eigenstates. Each pair of these parameters affects the total solar neutrino spectrum differently, which can give rise to the energy dependence in the ratio between the observed and the predicted neutrino fluxes in different detectors. Using the measured rates in the radiochemical (^{37}Cl and ^{71}Ga) experiments, the solar zenith angle distribution from the Super-Kamiokande experiment, and the day and night energy spectra from the SNO experiment, a global statistical analysis can then be performed to determine the $(\Delta m^2, \tan^2 \theta)$ pair that best describes the data²⁹. The best-fit parameters²¹

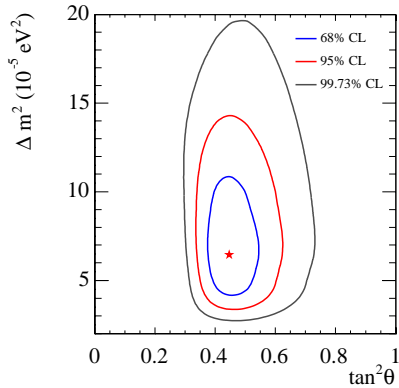


Figure 6. Global neutrino oscillation analysis of solar neutrino data. The solar neutrino data include SNO-I day and night spectra, SNO-II day and night CC spectra and ES and NC fluxes, the SK-I solar zenith spectra, and the rate measurements from the ^{37}Cl (Homestake) and ^{71}Ga (SAGE, GALLEX, GNO) experiments.

are found in the so-called “Large Mixing Angle” (LMA) region:

$$\begin{aligned} \Delta m^2 &= 6.5_{-2.3}^{+4.4} \times 10^{-5} \text{eV}^2 \\ \tan^2 \theta &= 0.45_{-0.08}^{+0.09}. \end{aligned}$$

There are two implications to these results. First, maximal mixing (i.e. $\tan^2 \theta = 1$) is ruled out at very high significance. This is in contrary to the atmospheric neutrino sector, where maximal mixing is the preferred scenario. Second, because the “dark-side” ($\tan^2 \theta > 1$) is also ruled out, a mass hierarchy of $m_2 > m_1$ is implied.

6 KamLAND

Previous reactor $\bar{\nu}_e$ oscillation experiments, with reactor-detector distances (“baselines”) ranging from ~ 10 m to ~ 1 km, did not observe any $\bar{\nu}_e$ disappearance³⁰. If CPT is conserved and matter-enhanced neutrino oscillation is the underlying mechanism for the observed flavor transformation in solar neutrinos, one would expect a significant fraction of the reactor $\bar{\nu}_e$ s oscillating (primarily through vacuum oscillation) into another fla-

vor at a baseline of 100 to 200 km. The Kamioka Liquid scintillator Anti-Neutrino Detector (KamLAND) experiment²² has a unique geographic advantage over other previous reactor $\bar{\nu}_e$ experiments; it is surrounded by 53 Japanese power reactors with an average baseline of 180 km.

KamLAND is a 1000-tonne liquid scintillator detector located in the Kamioka mine in Japan. Its scintillator is a mixture of dodecane (80%), pseudocumene (1,2,4-Trimethylbenzene, 20%), and 1.52 g/liter of PPO (2,5-Diphenyloxazole). An array of 1325 17-inch-diameter PMTs and 554 20-inch-diameter PMTs are mounted inside the spherical containment vessel. Outside this vessel, an additional 225 20-inch-diameter PMTs act as a cosmic-ray veto counter.

KamLAND detects $\bar{\nu}_e$ s by the inverse β decay process $\bar{\nu}_e + p \rightarrow e^+ + n$, which has a 1.8 MeV kinematic threshold. The prompt signal E_{prompt} in the scintillator, which includes the positron kinetic energy and the annihilation energy, is related to the incident $\bar{\nu}_e$ energy $E_{\bar{\nu}_e}$ and the average neutron recoil energy \bar{E}_n by $E_{\bar{\nu}_e} = E_{\text{prompt}} + \bar{E}_n + 0.8$ MeV. The final state neutron is thermalized and captured by a proton with a mean lifetime of $\sim 200 \mu\text{s}$. The prompt signal and the 2.2-MeV γ emitted in the delayed neutron capture process form a coincident signature for the $\bar{\nu}_e$ signal.

Table 2 summarizes the two KamLAND reactor $\bar{\nu}_e$ rate measurements^{23,24} to-date. The exposure of the two measurements are 162 ton-years and 766 ton-years respectively. The null hypothesis that the observed $\bar{\nu}_e$ rates are statistical downward fluctuations is rejected at 99.95% and 99.998% confidence levels in the two measurements. KamLAND is the first experiment that observes reactor $\bar{\nu}_e$ disappearance.

If vacuum oscillation is responsible for the disappearance of reactor $\bar{\nu}_e$ s in KamLAND, then one might expect a distortion of the E_{prompt} spectrum. The measured

Table 2. Summary of KamLAND $\bar{\nu}_e$ rate measurements.

	First result ²³	Second result ²⁴
<i>Data Sets</i>		
Data span	Mar. 4, 2002 to Oct. 6, 2002	Mar. 9, 2002 to Jan. 11, 2004
Live days	145.1 live days	515.1 live days
Exposure	162 ton-year	766.3 ton-year
<i>Results</i>		
Expected signal	86.8 ± 5.6 counts	365.2 ± 23.7 counts
Background	1 ± 1 count	17.8 ± 7.3 counts
Observed signal	54 counts	258 counts
Systematic uncertainties	6.4%	6.5%
$\bar{\nu}_e$ disappearance C.L.	99.95%	99.998%

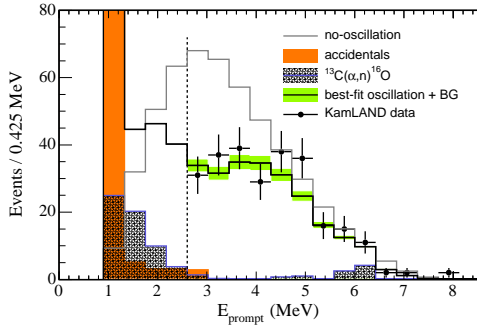


Figure 7. Prompt energy spectrum of $\bar{\nu}_e$ candidate events in the 766-ton-year KamLAND analysis. Also shown are the no-oscillation spectrum and the best-fit spectrum under the assumption of neutrino oscillation.

E_{prompt} spectrum is shown in Fig. 7. A fit of the observed E_{prompt} spectrum to a simple re-scaled, undistorted energy spectrum is excluded at 99.6%. Also shown in the figure is the best-fit spectrum under the assumption of neutrino oscillation. The allowed oscillation parameter space is shown in Fig. 8, and the best-fit parameters of this KamLAND-only analysis are²⁴

$$\Delta m^2 = 7.9_{-0.5}^{+0.6} \times 10^{-5} \text{eV}^2$$

$$\tan^2 \theta = 0.46.$$

Assuming CPT invariance, a global neutrino oscillation analysis can be performed on the solar neutrino results and the Kam-

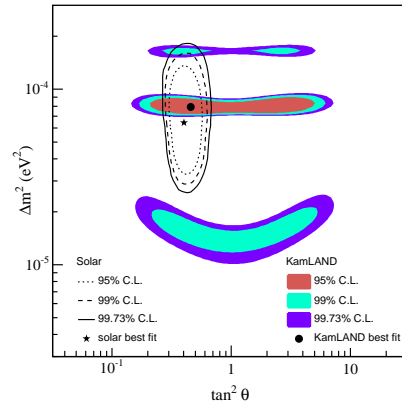


Figure 8. Neutrino oscillation parameter allowed region from the 766-ton-year KamLAND reactor $\bar{\nu}_e$ results (shaded regions) and the LMA region derived from solar neutrino experiments (lines).

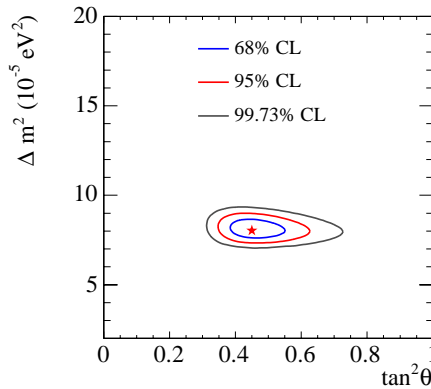


Figure 9. Global neutrino oscillation analysis of solar neutrino experiments and KamLAND. The best fit point is at $(0.45_{-0.07}^{+0.09}, 8.0_{-0.4}^{+0.6} \times 10^{-5} \text{eV}^2)$.

LAND results. The allowed parameter space is shown in Fig. 9. The best-fit parameters in this global analysis are²¹

$$\begin{aligned}\Delta m^2 &= 8.0_{-0.4}^{+0.6} \times 10^{-5} \text{eV}^2 \\ \tan^2 \theta &= 0.45_{-0.07}^{+0.09}.\end{aligned}$$

One immediately notices the complementarity of reactor anti-neutrino and solar neutrino experiments. The former restricts Δm^2 , whereas the latter restricts $\tan^2 \theta$ in an orthogonal manner.

7 Future Experimental Solar Neutrino Program

In the next several years, both running solar neutrino experiments SNO and Super-Kamiokande have an ambitious physics program.

The three-flavor mixing matrix element U_{e2} can be written³¹ as $\cos \theta_{13} \sin \theta_{12}$, which approximately equals $\sin \theta$ for two-flavor solar neutrino oscillation when θ_{13} is small and when Δm^2 from the solar neutrino sector is much less than that from the atmospheric neutrino sector. For oscillation parameters in the LMA region, the MSW effect can result in ${}^8\text{B}$ neutrinos emerging from the Sun essentially as a pure ν_2 state. The SNO ϕ^{CC}/ϕ^{NC} ratio, a direct measure of ν_e survival probability, is also a direct measure of $|U_{e2}|^2$ ($\sim \sin^2 \theta$). Therefore, one of the primary goals of the SNO experimental program is to make a precision measurement of this fundamental parameter by improving on the CC and NC measurements.

The SNO experiment has entered the third phase (SNO-III) of its physics program. Thirty six strings of ${}^3\text{He}$ and 4 strings of ${}^4\text{He}$ proportional counters have been deployed on a 1-m square grid in the D_2O volume. In SNO-I and SNO-II, the extracted CC and NC fluxes are strongly anti-correlated (the correlation coefficient is -0.53 in SNO-II). This anticorrelation is a significant fraction of the total flux uncertainties. By introduction this

array of ${}^3\text{He}$ proportional counters, NC neutrons are detected by $n + {}^3\text{He} \rightarrow p + {}^3\text{H}$; whereas the Cherenkov light from the CC electrons are recorded by the PMT array. This physical separation, as opposed to a statistical separation of the CC and NC signals in SNO-I and SNO-II, will allow a significant improvement in the precision of the CC and the NC fluxes. Table 3 summarizes the uncertainties in the CC and NC flux measurements in SNO-I and SNO-II, and the projected uncertainties for the corresponding measurements in SNO-III.

Because the ${}^3\text{He}$ proportional counter array “removes” Cherenkov light signals from NC interactions, it allows for a search of CC electron spectral distortion at an analysis threshold of $T_{\text{eff}} = 4$ to 4.5 MeV. The distortion effects are enhanced at this threshold when compared to those analyses at higher thresholds in SNO-I and SNO-II.

The Super-Kamiokande is scheduled for a detector upgrade from October 2005 to March 2006. After this upgrade, the detector will return to the same photocathode coverage in SK-I. The primary physics goal of the SK-III solar neutrino program is to search for direct evidence of the MSW effect. With the improvements made to the trigger system in SK-II and the anticipated increase in photocathode coverage, the SK-III detector will be able to push the analysis threshold down to $E \sim 4$ MeV.

Figure 10 shows the projected SK-III sensitivity to observing spectral distortion in its solar neutrino signal. In this figure, the sensitivities of several combinations of $(\Delta m^2, \sin^2 \theta)$ in the LMA region allowed by solar neutrino measurements (c.f. Fig. 6) are shown. It is possible to discover MSW-induced spectral distortion at $> 3\sigma$ after several years of counting.

Future solar neutrino experiments focus on detecting the low energy pp neutrinos ($E_\nu < 0.42$ MeV), ${}^7\text{Be}$ neutrinos ($E_\nu = 0.86$ MeV, BR=90%), pep neutrinos ($E_\nu =$

Table 3. Uncertainties in the CC and NC fluxes in SNO-I, SNO-II and SNO-III. The SNO-III entries are projected uncertainties for 1 live year of data. The total uncertainties are the quadratic sum of the statistical and systematic uncertainties.

	SNO-I		SNO-II		SNO-III	
	$\Delta\phi^{CC}/\phi^{CC}$	$\Delta\phi^{NC}/\phi^{NC}$	$\Delta\phi^{CC}/\phi^{CC}$	$\Delta\phi^{NC}/\phi^{NC}$	$\Delta\phi^{CC}/\phi^{CC}$	$\Delta\phi^{NC}/\phi^{NC}$
Systematic	5.3	9.0	4.9	7.3	3.3	5.2
Statistical	3.4	8.6	3.7	4.2	2.2	3.8
Total	6.3	12.4	6.1	8.4	4.0	6.4

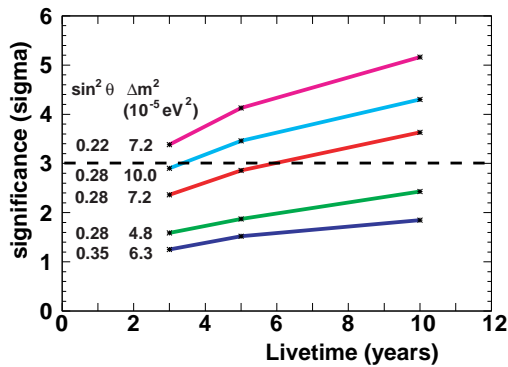


Figure 10. Projected sensitivity to spectrum distortion for SK-III. Each curve represents the significance for observing spectral distortion with the labeled mixing parameters.

1.44 MeV), or neutrinos from the CNO cycle. These experiments are subdivided into two broad classes: ν_e -only detection mechanism through ν_e charged-current interaction with the target nucleus; and νe elastic scattering which measures an admixture of ν_e , ν_μ and ν_τ . The pp neutrino experiments seek to make high precision measurement of the pp neutrino flux and to constrain the flux of sterile neutrinos. The ${}^7\text{Be}$ and the pep neutrino experiments seek to map out the ν_e survival probability in the vacuum-matter transition region. Figure 11 shows this transition region³². Although certain non-standard interaction (NSI) models³³ can match the survival probability in the pp and the ${}^8\text{B}$ energy regimes, they differ substantially from the MSW prediction in the ${}^7\text{Be}$ and pep energy regimes ($E_\nu \sim 1 - 2$ MeV).

Table 4 is a tabulation of future solar neutrino experiments (adopted from Nakahata³⁴). Most of these experiments are in proposal stage; but two liquid scintillator experiments, Borexino and KamLAND, will come online for ${}^7\text{Be}$ solar neutrino measurements in the next year. The construction of Borexino is complete, and it is waiting for authorization to fill the detector with liquid scintillator. The purification system of the KamLAND experiment is being upgraded in order to achieve an ultra-pure liquid scintillator for the ${}^7\text{Be}$ neutrino measurement.

For other future solar experiments, a summary of their current status can be found in the supplemental slides of this conference talk³⁵.

8 Future Experimental Reactor Anti-neutrino Program

The future reactor anti-neutrino program is focused on determining the neutrino mixing angle θ_{13} . This is the only unknown angle in the neutrino mixing matrix, and its current upper limit is $\sin^2(2\theta_{13}) < 0.2$ (90% C.L.)³⁶.

Although there are ongoing efforts in developing accelerator-based θ_{13} measurements by searching for $\nu_\mu \rightarrow \nu_e$ appearance, such long baseline measurements can be affected by matter effects. The determination of θ_{13} in these appearance experiments is complicated by the degeneracy of mixing parameters (e.g. θ_{23}). A reactor-based θ_{13} measurement can complement accelerator-based ex-

Table 4. Future solar neutrino experiments. Those experiments identified with an asterisk have been funded for the full scale detector.

Experiment	ν source	Reaction	Detector
<i>Charged-Current Detectors</i>			
LENS	pp	$\nu_e^{115}\text{In} \rightarrow e^{115}\text{Sn}, e, \gamma$	15 tons of In in 200-ton liquid scintillator
Lithium	pep, CNO	$\nu_e^7\text{Li} \rightarrow e^7\text{Be}$	Radiochemical, 10 ton lithium
MOON	pp	$\nu_e^{100}\text{Mo} \rightarrow e^{100}\text{Tc}(\beta)$	3.3 ton ^{100}Mo foil + plastic scintillator
<i>νe Elastic Scattering Detectors</i>			
Borexino*	^7Be	$\nu e \rightarrow \nu e$	100 ton liquid scintillator
CLEAN	$pp, ^7\text{Be}$	$\nu e \rightarrow \nu e$	10 ton liquid Ne
HERON	$pp, ^7\text{Be}$	$\nu e \rightarrow \nu e$	10 ton liquid He
KamLAND*	^7Be	$\nu e \rightarrow \nu e$	1000 ton liquid scintillator
SNO+	pep, CNO	$\nu e \rightarrow \nu e$	1000 ton liquid scintillator
TPC-type	$pp, ^7\text{Be}$	$\nu e \rightarrow \nu e$	Tracking electron in gas target
XMASS	$pp, ^7\text{Be}$	$\nu e \rightarrow \nu e$	10 ton liquid Xe

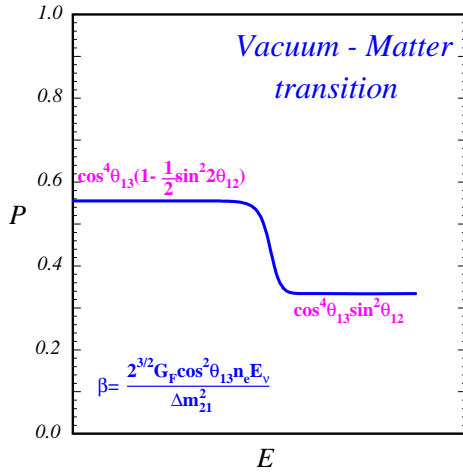


Figure 11. Vacuum-matter transition of ν_e survival probability. In the pp neutrino regime, the survival probability is approximately $(1 - \frac{1}{2} \sin^2 2\theta_{12})$ (for $\theta_{13} \ll 1$). In the energy regime where ^8B neutrinos are observed, the survival probability is approximately $\sin^2 \theta_{12}$. Non-standard interactions (NSI) predict a substantially different energy dependence in the transition region, and future ^7Be and the pep neutrinos experiments can be used to discriminate these NSI models from the MSW scenario.

periments by removing these intrinsic ambiguities. In a reactor-based measurement, one searches for $\bar{\nu}_e$ flux suppression and spectral distortion of the prompt positron signal at different baselines.

The general configuration of such a reactor-based experiment consists of at least two or more detectors: one is placed at a distance of <0.5 km, and the other at 1-2 km. The *near* detector is used to normalize the reactor $\bar{\nu}_e$ flux, while the *far* detector is used to search for rate suppression and spectral distortion. The baseline of the far detector, ~ 2 km, is the distance where the survival probability reaches its first minimum. In order to shield the detectors from muon spallation backgrounds, these detectors require overhead shielding. For these experiments, a $<\sim 1\%$ error budget is required in order to reach a $\sin^2 2\theta_{13}$ sensitivity of $<\sim 0.01$.

In addition to θ_{13} measurements, these experiments can also make contributions in measuring the Weinberg angle $\sin \theta_W$ (at $Q^2 = 0$), and in investigating the nature of neutrino neutral-current weak coupling. The precision in θ_{12} can also be improved by a reactor anti-neutrino experiment with a base-

line of 50 to 70 km³⁷.

Table 5 is a tabulation of the proposed reactor θ_{13} experiments³⁸. More details on the status of these experiments can be found in the supplemental slides of this talk³⁵.

9 Conclusions

After nearly four decades, the solar neutrino deficit problem is finally resolved. There are now strong evidences for neutrino oscillation from solar neutrino and reactor anti-neutrino experiments. SNO, Super-Kamiokande and KamLAND will improve the precision of the neutrino oscillation parameters. Future solar neutrino experiments will provide high precision tests of the solar model calculations, and will probe the energy dependence of neutrino oscillation. Future reactor anti-neutrino experiments will attempt to measure the unknown mixing angle θ_{13} . Once the magnitude of this angle is known, a new arena of CP studies may be opened up in the neutrino sector in the future.

Acknowledgments

The author thanks the conference organizers for the invitation to speak; and E. Blucher, M. Chen, P. Decowski, H. Ejiri, R. Hazama, K. Ishii, R. Lanou, T. Lasserre, K.-B. Luk, D. McKinsey, M. Nakahata, R. Raghavan, F. Suekane, R. Svoboda, and Y. Takeuchi for providing much of the background information in this talk and proceedings.

References

1. J. N. Bahcall, M. Pinsonneault, S. Basu, *Astrophys. J.* **555**, 999 (2001).
2. J. N. Bahcall and M. H. Pinsonneault, *Phys. Rev. Lett.* **92**, 121301 (2004).
3. J. N. Bahcall, A. M. Serenelli, and S. Basu, astro-ph/0412440.
4. A. S. Brun, S. Turck-Chièze, and J. P. Zahn, *Astrophys. J.* **525**, 1032 (1999).
5. S. Turck-Chièze *et al.*, *Ap. J. Lett.* **555** (2001).
6. S. Turck-Chièze *et al.*, *Phys. Rev. Lett.* **93**, 221102 (2004).
7. B. T. Cleveland *et al.* [Homestake Collaboration], *Astrophys. J.* **496**, 505 (1998).
8. J. N. Abdurashitov *et al.* [SAGE Collaboration], *J. Exp. Theor. Phys.* **95**, 181 (2002).
9. W. Hampel *et al.* [GALLEX Collaboration], *Phys. Lett. B* **447**, 127 (1999).
10. M. Altmann *et al.* [GNO COLLABORATION Collaboration], *Phys. Lett. B* **616**, 174 (2005).
11. S. Fukuda *et al.* [Super-Kamiokande Collaboration], *Nucl. Instr. Meth. A* **501**, 418 (2003).
12. S. Fukuda *et al.* [Super-Kamiokande Collaboration], *Phys. Rev. Lett.* **86**, 5651 (2001).
13. S. Fukuda *et al.* [Super-Kamiokande Collaboration], *Phys. Rev. Lett.* **86**, 5656 (2001).
14. M. B. Smy *et al.* [Super-Kamiokande], *Phys. Rev. D* **69** 011104 (2004).
15. Y. Fukuda *et al.* [Kamiokande Collaboration], *Phys. Rev. Lett.* **77**, 1683 (1996).
16. J. Boger *et al.* [SNO Collaboration], *Nucl. Instr. and Meth. A* **449**, 172 (2000).
17. Q. R. Ahmad *et al.* [SNO Collaboration], *Phys. Rev. Lett.* **87**, 071301 (2001).
18. Q. R. Ahmad *et al.* [SNO Collaboration], *Phys. Rev. Lett.* **89**, 011301 (2002).
19. Q. R. Ahmad *et al.* [SNO Collaboration], *Phys. Rev. Lett.* **89**, 011302 (2002).
20. S. N. Ahmed *et al.* [SNO Collaboration], *Phys. Rev. Lett.* **92**, 181301 (2004).
21. B. Aharmim *et al.* [SNO Collaboration], arXiv:nucl-ex/0502021.

Table 5. Proposed reactor anti-neutrino experiments for measuring θ_{13} .

Experiment	Location	Baseline (km)		Overburden (m.w.e.)		Detector size (tons)		$\sin^2(2\theta_{13})$ sensitivity (90% C.L.)
		Near	Far	Near	Far	Near	Far	
Angra dos Reis	Brazil	0.3	1.5	200	1700	50	500	$<\sim 0.01$
Braidwood	USA	0.27	1.51	450	450	65×2	65×2	$<\sim 0.01$
Double Chooz	France	0.2	1.05	50	300	10	10	$<\sim 0.03$
Daya Bay	China	0.3	1.8-2.2	300	1100	50	100	$<\sim 0.01$
Diablo Canyon	USA	0.4	1.7	150	750	50	100	$<\sim 0.01$
KASKA	Japan	0.4	1.8	100	500	8	8	$<\sim 0.02$
Kr2Det	Russia	0.1	1.0	600	600	50	50	$<\sim 0.03$

22. A. Suzuki, talk at the XVIII International Conference on Neutrino Physics and Astrophysics, Takayama, Japan, (1998).
23. K. Eguchi *et al.* [KamLAND Collaboration], *Phys. Rev. Lett.* **90**, 021802 (2003).
24. T. Araki *et al.* [KamLAND Collaboration], *Phys. Rev. Lett.* **94**, 081801 (2005).
25. S. P. Mikheyev and A. Yu. Smirnov, *Sov. J. Nucl. Phys.* **42** 913 (1985); L. Wolfenstein, *Phys. Rev.* **D17** 2369 (1978).
26. Super-Kamiokande results presented in this paper are preliminary results provided by the collaboration. Since this conference, the Super-Kamiokande collaboration has published a full summary of its SK-I results in J. Hosaka *et al.*, arXiv:hep-ex/0508053.
27. H. H. Chen, *Phys. Rev. Lett.* **55**, 1534 (1985).
28. G.L. Fogli, E. Lisi, A. Marrone, and A. Palazzo, *Phys. Lett. B* **583** 149 (2004).
29. Examples of such global analyses include J.N. Bahcall, M.C. Gonzalez-Garcia and C. Peña-Garay, *JHEP* **08**, 016 (2004); A. B. Balantekin and H. Yüksel, *Phys. Rev. D* **68**, 113002 (2003); A. Bandyopadhyay, S. Choubey, S. Goswami, S. T. Petcov, and D. P. Roy, *Phys. Lett. B* **583**, 134 (2004); G. L. Fogli *et al.* *Phys. Rev. D* **66**, 053010 (2002); P. C. de Holanda and A. Yu. Smirnov, *Astropart. Phys.* **21**, 287 (2004).
30. A comprehensive review of reactor neutrino oscillation experiments, prior to the KamLAND experiment, can be found in C. Bemporad, G. Gratta, and P. Vogel, *Rev. Mod. Phys.* **74**, 297 (2002).
31. Z. Maki, N. Nakagawa, and S. Sakata, *Prog. Theor. Phys.* **28**, 870 (1962); V. Gribov and B. Pontecorvo, *Phys. Lett. B* **28**, 493 (1969).
32. J.N. Bahcall and C. Peña-Garay, *JHEP* **11**, 004 (2003)
33. O. G. Miranda, M. A. Tortola and J. W. F. Valle, *Nucl. Phys. Proc. Suppl.* **145**, 61 (2005); A. Friedland, C. Lunardini and C. Pena-Garay, *Phys. Lett. B* **594**, 347 (2004).
34. M. Nakahata, *Nucl. Phys. Proc. Suppl.* **145**, 23 (2005).
35. The conference website is <http://www.uu.se/LP2005>.
36. M. Apollonio *et al.* [CHOOZ Collaboration], *Eur. Phys. J. C* **27**, 331 (2003).
37. A. Bandyopadhyay, S. Choubey, S. Goswami and S. T. Petcov, *Phys. Rev. D* **72**, 033013 (2005)
38. E. Abouzaid *et al.*, *Report of the APS Neutrino Study Reactor Working Group*,

For Publisher's use

<http://www.aps.org/neutrino> (2004).

DISCUSSION

Jonathan Rosner (U. of Chicago, USA):

Can you say more about the proposal to put liquid scintillator in SNO?

Alan Poon : The main objectives of this proposed experiment are to measure the *pep* neutrino flux and to search for geo-neutrinos. The *pep* measurement will probe the vacuum-matter transition that I discussed in the talk.

The project is still in an early proposal stage. There are a number of technical problems that need to be resolved before its realisation. For example, the compatibility of the liquid scintillator and the acrylic vessel has to be established; the longevity of the current photomultiplier tube mounting structure, which was designed to have a life span of 10 years in ultra-pure water, has to be evaluated; and the optical response of the liquid scintillator has to be established.

Peter Rosen (DOE, USA): A comment about MSW. If you restrict your analysis to 2 flavors, then the fact that the solar ν_e survival probability is less than 1/2 is evidence for MSW. Pure in-vacuum oscillation give a survival probability greater than or equal to 1/2. Secondly, the best chance to see a day/night effect is to have a detector at the equator. This maximizes the path of the neutrino through matter, and through the densest part of the Earth.

Alan Poon : Thank you for your comment. Because of time constraint, I did not have enough time to discuss this point further in my talk. It is true that even though we have not directly observed MSW effect, there are very strong indirect evidence that it is the underlying mechanism for neutrino flavor transformation in solar neutrinos. Fogli *et al.*

showed that the null hypothesis of no MSW effect in the solar neutrino results is rejected at more than 5σ .